ESCUELA TÉCNICA SUPERIOR DE INGENIEROS
INDUSTRIALES Y DE TELECOMUNICACIÓN

UNIVERSIDAD DE CANTABRIA

Trabajo Fin de Grado

CONTRIBUCIÓN AL DISEÑO DE SISTEMAS MICROFLUÍDICOS PARA LA SEPARACIÓN DE PARTÍCULAS MAGNÉTICAS

(Contribution to the design of microfluidic systems for the separation of magnetic particles)

Para acceder al Título de

Graduado/a en Ingeniería Química

Autor: Cristina González Fernández

Content

1. Introduction

Biomolecules separation is of broad importance in many biological and medical applications due to either their added value or the need of separation by their hazardous properties. Recently, the removal of toxic substances from blood has received special attention from the scientific community. These substances include biotoxins, microorganisms, toxic chemicals, drugs, heavy metal ions or radioactive toxins, which can cause diseases or death. In fact, for a number of clinical conditions such as intoxication, bacteraemia or autoimmune diseases, the removal of the disease-causing agents from blood can be considered as the most direct conceivable treatment. [1,2]

As depicted in Figure 1, several methods have been employed for the separation of those toxic substances from different biological fluids such as blood, plasma, dialysis fluids, etc.[1,3]

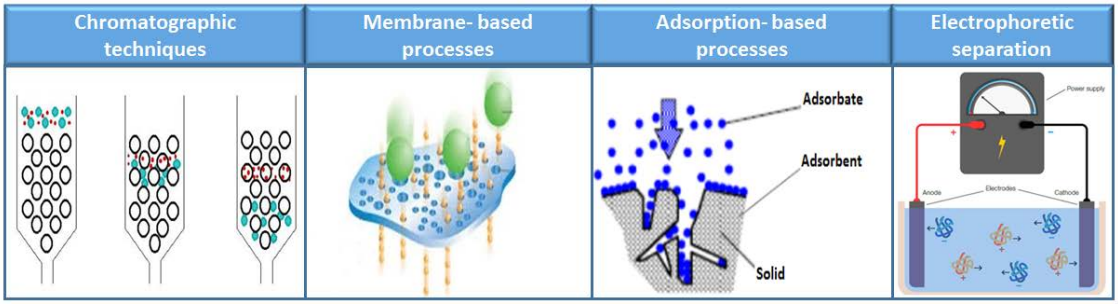

Figure 1. Conventional technologies for the removal of toxic substances from biological fluids. [4-7]

Chromatographic methods are able to separate in an efficient way biomolecules in pure form after the pre-treatment of the initial sample. However, they are relatively time-consuming and exhibit several associated drawbacks such as: high-pressure packing, high pressure drop in the column and slow intra-bead diffusion of solutes. Besides, they require large sample volumes.[8,9] Regarding to electrophoretic separations, some of them are only applicable to ionic or ionogenic materials and others are not enough efficient for trace separations.[10,11]

During ultrafiltration operation, fouling and concentration polarization phenomena take place thus declining the flux and often selectivity. Moreover, ultrafiltration requires large differences in size between the product and contaminant and the membrane exhibits an uncontrollable sieving/selectivity. Although hemodialysis and hemofiltration remove low molecular weight compounds from blood, hemofiltration is a high cost therapy and cannot remove effectively small protein-bound solutes. In addition, during hemodialysis, toxic substances can enter from the contaminated dialysis fluid to the patient's blood by backfiltration or backdiffusion. As for hemodiafiltration, some systems can only handle small fluid volumes and intravenous solutions cost and clotting within the hemodiafilter are crucial issues.[1,3,12-18]

Despite hemoperfusion and hemoadsorption can be appropriate for the separation of high molecular weight compounds, the former has associated potential side effects such as unspecific protein adsorption, loss of blood cells and possible activation of coagulation and inflammation pathways during operation. On the other hand, the later presents poor biocompatibility which is evidenced by severe thrombocytopenia and leukopenia.[3,19]

Compared to the aforementioned separation processes, the use of magnetic nanoparticles (MNPs), also called magnetic beads, as adsorbents for bio-separations or detoxification of biological fluids exhibits significant benefits for removing toxic compounds either for patient treatment or diagnosis purposes. This is due to their enhanced properties, i.e high specific surface area, chemical stability, low intraparticle diffusion rate, high loading capacity, biocompatibility, etc. Such properties result to a lower dose and faster kinetics in comparison with conventional hemoadsorbent materials, thus reducing costs, producing less contamination and improving the selectivity of the process.[2,20] Besides, they can be synthesized in a wide range of sizes (from a few to tens of nanometers) with a narrow size distribution.[21] The small size, high surface-to-volume ratio and high mobility of MNPs lead to short diffusion distances and therefore, the binding efficiencies are increased even for high molecular weight compounds.[3]

On the other hand, magnetic interactions are normally not affected by surface charges, pH, ionic concentrations or temperature. They are also considerably faster than other methods, and enable the direct isolation of the target biomaterial from samples (blood, bone marrow, and tissue homogenates). Owing to the relatively low intrinsic magnetic susceptibility of biomaterials, there is a considerable contrast between tagged and untagged material, which leads to a high degree of selectivity. Also, the interaction between the applied field and the magnetically labeled material is facilitated by the relatively low permeability of the medium.[22,23]

The removal of toxins from biological fluids is challenging since the characteristics of the target toxin need to be identified in order to design the selective antitoxin nanoadsorbent. The MNPs employed for toxin sequestration are generally based on composites, with a diameter in the nanometer scale, in which several materials are combined with the objectives of maximizing the removal capacity of the system and minimizing the unspecific adsorption of the other components from the biological fluid, thus maintaining the functionality of the biological fluid that needs to be treated. Particles with high specific surface areas represent the best configuration for the maximization of surface functionality and capacity for toxin removal, as well as for the reduction of the material dosage. Thus, small particles are ideal for such applications since surface area inversely scales with particle size.[2] Figure 2 illustrates the most important constituents of the MNPs used as detoxification agents.

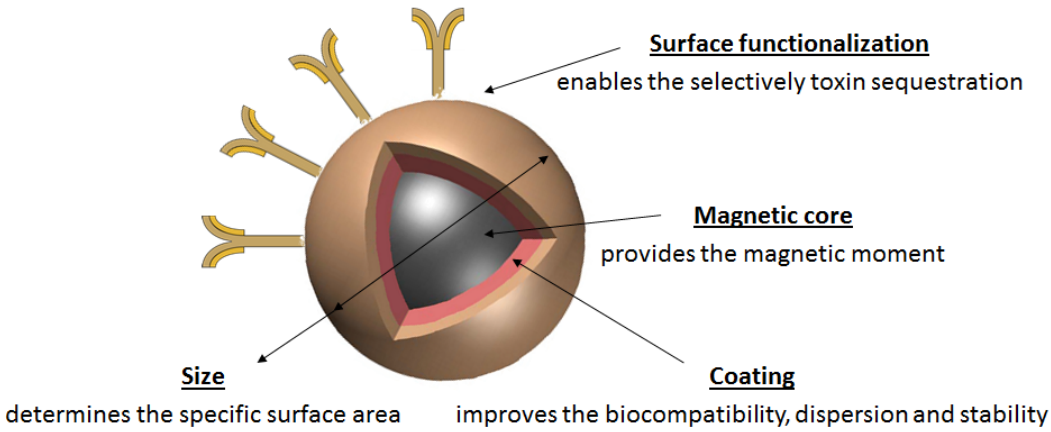

Figure 2. Schematic representation of the MNPs employed for the detoxification of biological fluids[2]

The inner core of the particle provides the magnetic aspect of the composite and is usually made from a ferromagnetic nanomaterial. Among them, iron oxides (magnetite or maghemite) are non-toxic, have been approved for in vivo use as toxin sequestering materials and provide sufficient magnetic moment to the particles. The core is embedded in a matrix that improves biocompatibility, dispersion and stability against corrosion and oxidation. These coatings are mainly based on organic polymers, inorganic metals or oxides. Since the MNPs should recognize a specific target (toxins, microorganisms, etc.), the resulting composite bead needs to be functionalized by anchoring specific antitoxin groups on its surface that are specifically tailored for each application and care should be taken to avoid the unspecific adsorption of other biomolecules onto the particle surface and thus limiting the treatment effectiveness.[2,20]

The use of MNPs for therapy against several diseases is extended to both *in vivo* and *ex vivo* applications. However, since the long term risks and possible side effects associated with the *in vivo* use of MNPs are not yet completely understood, an extracorporeal setting is preferred as it prevents MNPs from entering the body and from its accumulation.[2,3]

Despite offering the advantages detailed above, the pathogen-loaded particles need to be removed from the fluid when the adsorption stage is concluded.[3] Taking advantage of their superparamagnetic behavior, these particles can be separated from complex solutions by magnetic means.[20]

Magnetic particle sequestration can be integrated into microfluidic systems, which leads to the development of microfluidic magnetophoretic separation devices (MSDs). MSDs are the best candidates for the separation of beads at small scale applications because they are highly efficient, portable and exhibit rapid selective separation. Also, they can be manufactured with low cost because of the use of inexpensive materials and cost-effective manufacturing processes. Furthermore, this technology allows the sequestration of a non-magnetic substance (toxin, microorganism or toxic chemicals) through magnetic means.[2,20]

The use of microfluidics for that purpose stems from its potential advantages both from a technical and economical point of view. Microfluidics is an emerging state-of-the-art technology that handles small volumes of liquids (10^{-9} to 10^{-18} L) in networks of channels with dimensions of 5–500 µm (microchannels). It also allows to reduce the consumption of sample and reagent in several MNPs bioapplications such as diagnosis or clinical assays, which leads to significant cost and waste production reduction.

When the dimensions of the fluidics structures are scale down to the micrometer region, the surface to volume ratio of the fluids involved increases dramatically, and surface effects start to dominate volume effects. Consequently, the mass and heat transfer and the interfacial phenomena are enhanced owing to the high surface-area-to-volume-ratio of microfluidic devices. On the other hand, the reduced dimensions lead to well-defined flow characteristics, as the flow is strictly laminar and turbulence can only appear in very limited regions around sharp edges. This laminar flow profile inside the microchannel would ideally enable neighboring coflowing miscible fluids with no apparent turbulent mixing when several fluid streams are involved in the process. Thus, adjacent streams of miscible fluids flow through the microchannel side-by-side in the laminar regimen, and mixing only takes place by diffusion at the interface of the streams or by special designed fluidic mixing elements.[20,24-26]

Microfluidics has associated high throughput due to parallelization (scale out). and is an excellent example of process intensification due to their low fabrication cost and reagent consumption, small form factors for safe operation in a controlled environment and its capability of integrate multiple basic steps onto one chip (known as lab-on-a-chip(LOC) or micro-total analysis system (µ-TAS)).[26-28] Another area of biotechnology that has commercially benefited from microfluidic technologies is Rapid point-of-care (POC) diagnostics.[29] Furthermore, the integration and the mass-fabrication capabilities of microfabrication technology make the application of microfluidics attractive from an economic point of view and their small sizes allow the installation of these systems in portable equipment with low power consumption. [24,27]

A schematic diagram of a lab-on-a-chip device is illustrated in Figure 3. As it can be noticed, LOC or μ-TAS devices can integrate miniaturized laboratory functions such as separation, washing, concentration, detection, lysis of bio-particles or PCR-like reactions (polymerase chain reaction).[29,30]

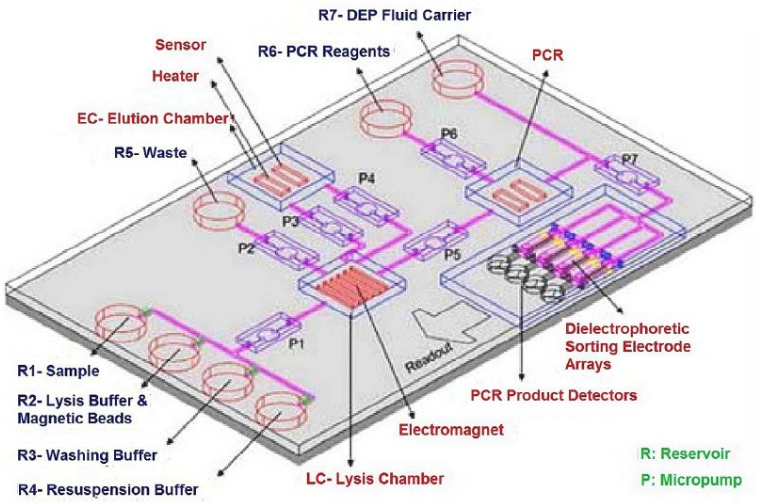

Figure 3. Functional diagram of Lab-on-a-chip device.[31]

The potential advantages of microfluidics and MNPs as detoxification agents detailed above are exploited in the design of MSDs to perform the separation of biomolecules from biological fluids by combining magnetophoretic and microfluidic techniques.

The MSDs can be classified into batch or continuous systems, which differ in the method by which the particles are collected.[20]In batch separators, the MNPs are accumulated on trapping elements using an external field, allowing their recovery when the field is removed. On the contrary, in the continuous mode, the forces acting on the particle are balanced so that they are concentrated in different outlets due to the deflection of their trajectories. [20]

The use of continuous systems can overcome some issues related to batch magnetic separators, such as the accumulation of beads on the walls which restricts fluid flow, decreasing the efficiency and capacity of the separator, or the non-specific entrapment of the biological fluid components in the capturing regions, degrading the quality of the treated solution.[2]

Besides, continuous separators enables a high level of the integration with previous processes (i.e. the adsorption of toxins) leading to a continuous detoxification system. Therefore, their use not only increases separation efficacy and throughput but also allows the integration of both stages into a seamless treatment scheme.[2] For both operating modes, several chip designs can be applied such as linear straight, L, T or Y-shaped [20]. In Figure 4, a continuous Y-shaped separator is depicted, where the biological fluid to be treated is blood. As it can be perceived, the blood with the loaded MNPs is injected through the upper inlet and the buffer solution through the lower one. Both fluids flow side-by-side across the microchannel as the toxins are removed along with the material, leading to a clean blood solution.

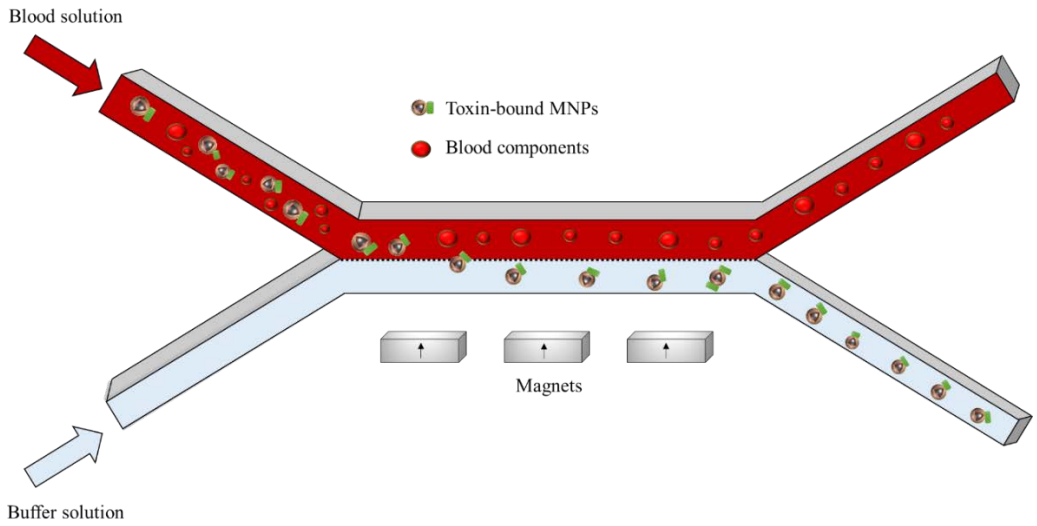

Figure 4. Schematic diagram of the continuous-flow Y-shaped magnetic separation.[2]

This separation stage can be integrated in a cleansing microdevice to perform the removal of toxic compounds from biological fluids employing MNPs as separation agents. This conceptual design is illustrated in Figure 5. It consists of two stages: i) adsorption of the target toxin using functionalized magnetic particles, and ii) magnetic recovery of the particles after the treatment.

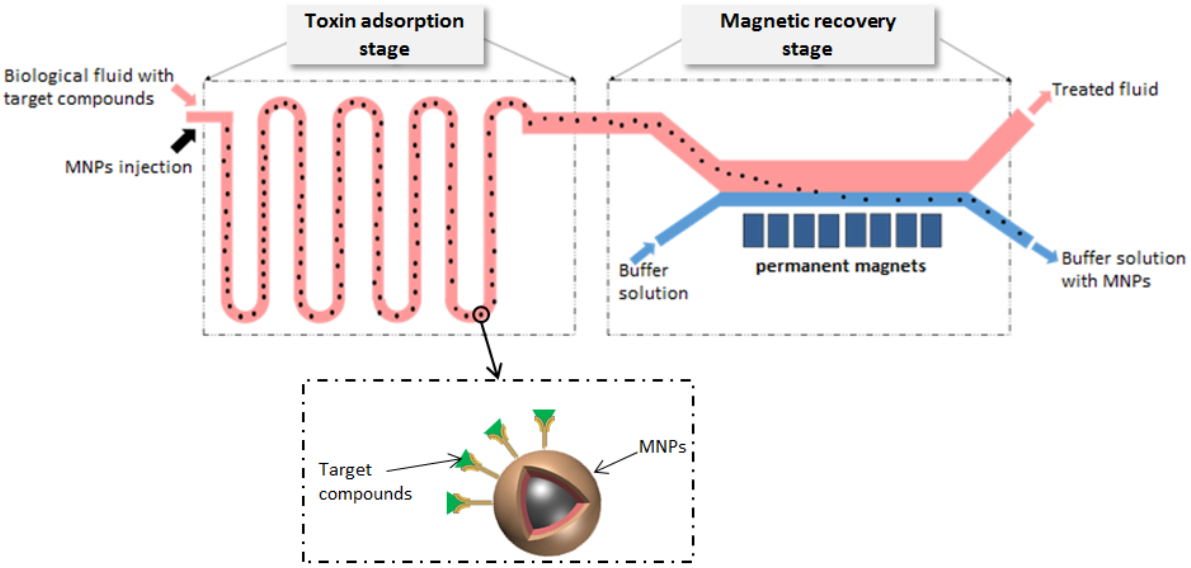

Figure 5. Preliminary design of the microfluidic device proposed for the detoxification of biological fluids.

In the proposed system, the functionalized MNPs are injected into the microdevice and they bind to the target compounds, adsorbing them to their surface.[3] The objective of the adsorption stage is that, the compounds with an acceptable affinity to the functionalized surface are captured by specific ligand-receptor binding while other non-targeted compounds are not affected. The performance of this stage is determined by the target-ligand binding (binding site accessibility, specificity, contact time)[3]. Once the adsorption stage is concluded, the treated biological fluid with the loaded MNPs enters into the magnetic separation stage through the upper inlet and a buffer solution, which acts as a carrier fluid to collect the loaded MNPs, through the lower inlet as seen in Figure 5. Both phases flow side-by-side along the microchip. A permanent magnet arrangement located next to the separation chamber exerts a magnetic gradient perpendicularly to the flow direction that deflects the MNPs from the biofluid stream, dragging them away to the buffer stream where they are collected. As a result of the treatment, the treated fluid leaves the system through one outlet and the exhausted MNPs are eluted from the system contained in the buffer solution through the other outlet. Afterwards, the loaded MNPs could be regenerated by a desorption step. Thereby, the adsorbed molecules could be later analyzed, disposed or submitted for assay or forensics.

Taking advantage of the laminar flow profile inside the MSDs, the purification of biological fluids can be performed without suffering any loss or dilution of the components. However, a problem arises in keeping a constant interface between all the streams within the microdevice, which makes their collection at different outlets very difficult, especially when the streams are based on different fluids.[20]

In this context, this project aims to contribute to the design and development of continuous microfluidic-magnetophoretic separators for the removal of toxic substances from biological fluids. Particularly, this project is focused on the design of the magnetic separation stage to perform the recovery of loaded magnetic particles from the target biological fluid.

2. Objectives

This Final Degree Project has been carried out at the facilities of the Research Group Advanced Separation Processes (ASP) located in the Department of Chemical and Biomolecular Engineering of the University of Cantabria. This work contributes to a novel research line focused on the design of extracorporeal blood-cleansing devices for sepsis therapy, which is being developed in collaboration with Valdecilla Biomedical Research Institute (IDIVAL). This project has been supported by the Ministry of Education, Culture and Sport through a Research Initiation Grant that aims at promoting research activities between end-of-degree and master students.

Within this project, the analysis of the extracorporeal magnetic bioseparator proposed for the detoxification of blood solutions has been addressed. In order to achieve an adequate magnetic recovery stage, the design of the separation process must fulfill the following requirements: i) to recover the loaded MNPs from the fluid to be treated and to transfer them to the buffer solution, ii) to avoid the fluids intermixing as they flow across the microchannels, iii) to keep constant the blood properties by controlling the diffusion of its components to the buffer solution.

The general objective of the Final Degree Project is to analyze the behavior in terms of flow patterns and mass transfer of two fluids flowing in multiphasic magnetophoretic

microdevices. This objective deals with requirements (ii) and (iii) previously defined. To fulfill with the general objective, several specific objectives need to be achieved:

1. To develop optic analysis methods for the evaluation of fluids flow and mass transfer in multiphasic microdevices using fluorescence model compounds.

2. To select the operation conditions to guarantee an independent flow of the fluids flowing through the microchannel.

3. To select the operation conditions that minimize mass transfer phenomena between the fluids flowing through the bioseparator.

3. Materials and methods

3.1. Materials

The experiments were performed using an asymmetric Y-shaped microchip (Microliquid) made of SU8 (which is an epoxy based, negative, near-UV photoresist material)[32] using pyrex as substrate. The chip was placed in a holder fabricated on polymethyl methacrylate (PPMA) (Microliquid), which has four fluidic connections that allow the input and output of the fluid phases. Figure 6 shows the appearance of both the chip and the holder employed to carry out the experiments.

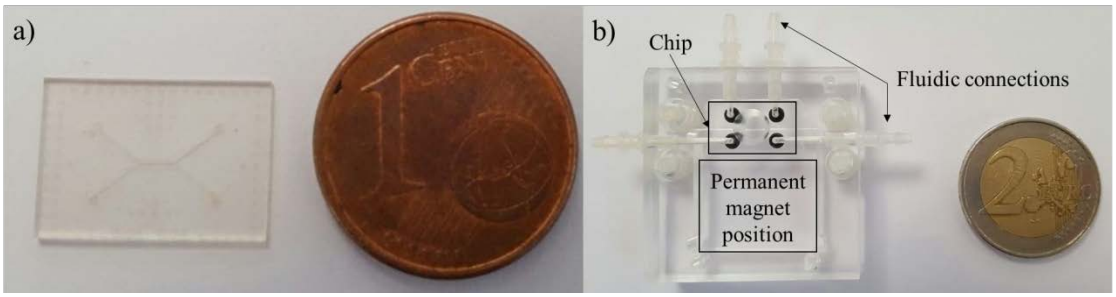

Figure 6. a) Microfluidic chip and b) separation chamber showing the chip with fluidic connections and magnet position.

Figure 7 illustrates a schematic representation as well as the dimensions of the Y-shaped chip used for the experiments.

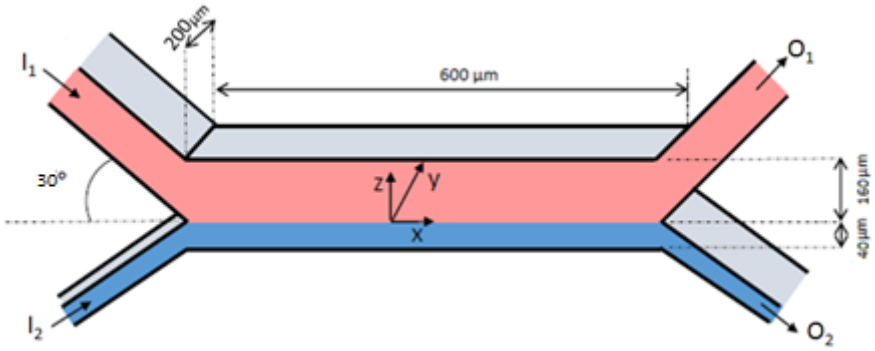

Figure 7. Schematic diagram of the continuous-flow magnetic separation microdevice.

As shown in Figure 7, the microchannel of rectangular section has two inlets (I_1 and I_2) and two outlets (O_1 and O_2) connected each of them by a Y junction. In the experiments, two syringe pumps (flow rate range from 5 pL·min^{-1} to 221 mL·min^{-1}; syringes volume from 0.5 µL to 140 mL; Legato 210 infuse/withdraw syringe pump, Kd Scientific) were used to control the flow rate at each inlet independently. A single syringe (Omnifix 5mL luer, BRAUN) was used for each pump. Fluids with two different characteristics were pumped into the two inlets: a) ultrapure water (w) (non fluorescent fluid) and fluorescein sodium (($C_{20}H_{10}Na_2O_5$), (Scharlau (extra pure)) in ultrapure water with a concentration of 60 ppm (f) (green fluorescent solution). Specifically, water entered the system through I_1 and fluorescein sodium solution through I_2 in all the experiments.

The use of fluorescein sodium for the experiments performance came from the similarity of the diffusion coefficient of that compound in water to the one of small ions or sugar molecules in plasma.[33] Also, the fluorescent properties of this compound allow their analysis with optic methods when it is irradiated with light with wavelengths values around 550 nm.

In a real application of this cleansing microdevice, it is expected that the treated biological fluid with the loaded MNPs will flow across the widest branch of the channel while the buffer solution across the thinnest one. This configuration will allow to reduce the volume of buffer solution required, thus increasing the blood flow rate inside the system and consequently, will make the process more efficient. Tygon tubing (ø=0.8mm,

Proquinorte) was employed for the fluidic connections, inserting the holder and the syringes connections in the tube.

Fluorescence intensity caused by the presence of fluorescein in the fluid phases inside the microchip was detected by fluorescence microscopy on a Nikon SMZ18 microscope (Zoom Ratio: 18:1; Zoom Range: 7.5–135x) equipped with a green fluorescence filter and a Jenoptik ProgRes C5 camera (Active area: 8.8 mm × 6.6 mm; Sensor resolution: 2580 × 1944 Pixel; Pixel size 3.4 µm × 3.4 µm) for detection. The microscope use in the experiments has a green excitation fluorescence filter capable of selective isolating fluorescence emissions. These color spectra are described quantitatively by wavelength of light from 500 to 570 nm.[34] Figure 8 shows the experimental setup used for the experiments.

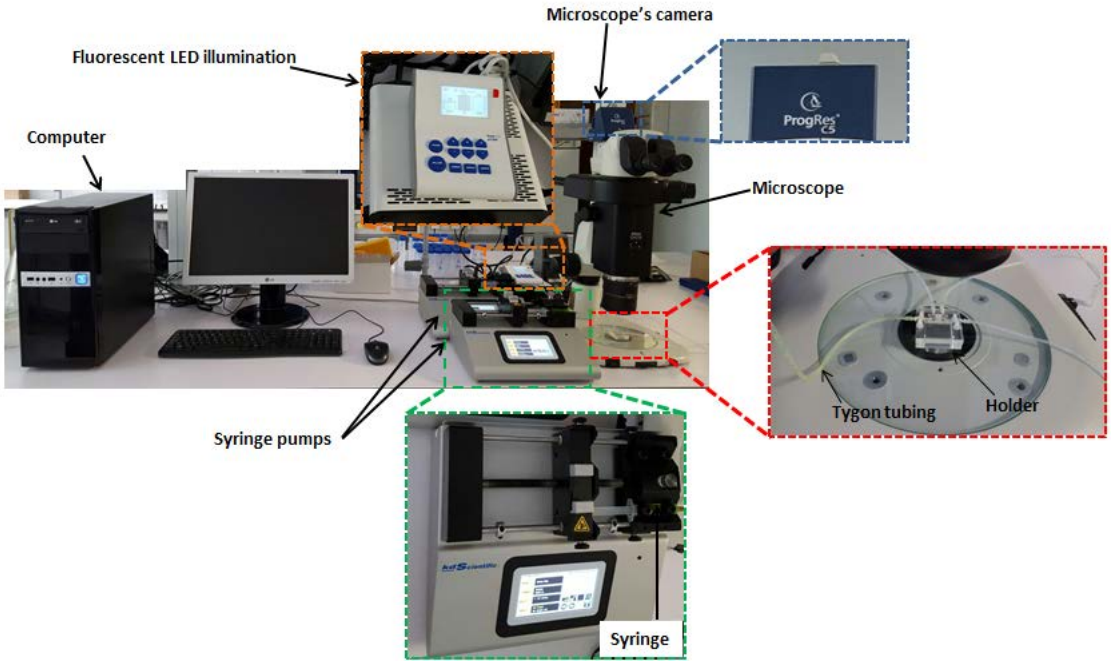

Figure 8. Experimental system.

Images were taken using the ProgRes® CapturePro software (CapturePro V2.10.0.0). The quantification of flow patterns and diffusion phenomena was performed by analyzing the photos taken with the microscope and the *Measurement* tool of the software "Image J" (Version 1.50e, NIH, USA).

3.2. Experimental methodology

The fluidic analysis aiming to describe the possible intermixing between both fluids (objective 2) and the fluorescein diffusion from one phase to the other (objective 3) were determined by measuring the dispersion of the fluorescence intensity (objective 1) as the fluids flow across the microchannels. In the experiments, after connecting the syringe pumps and the holder with the tygon tubes and focusing the microchip on the microscope, water and fluorescein sodium solutions were pumped into the microdevice. Photos were taken at different times in order to see how the flow was developed by using the software ProgRes® CapturePro. All of them were taken at 50X. The experimental procedure consisted of changing the flowrate of each fluid and different photos were taken in each experimental condition using the green fluorescence filter in the Nikon microscope. Afterwards, the photos were analyzed by using the Image J software.

The fluorescence intensities were measured in three different regions, which can be distinguished in each photo: the green-side branch (zone where it is expected that the fluorescein sodium solution flows), the black-side branch (zone where it is expected that the water flows) and the background. These regions are depicted in Figure 9.

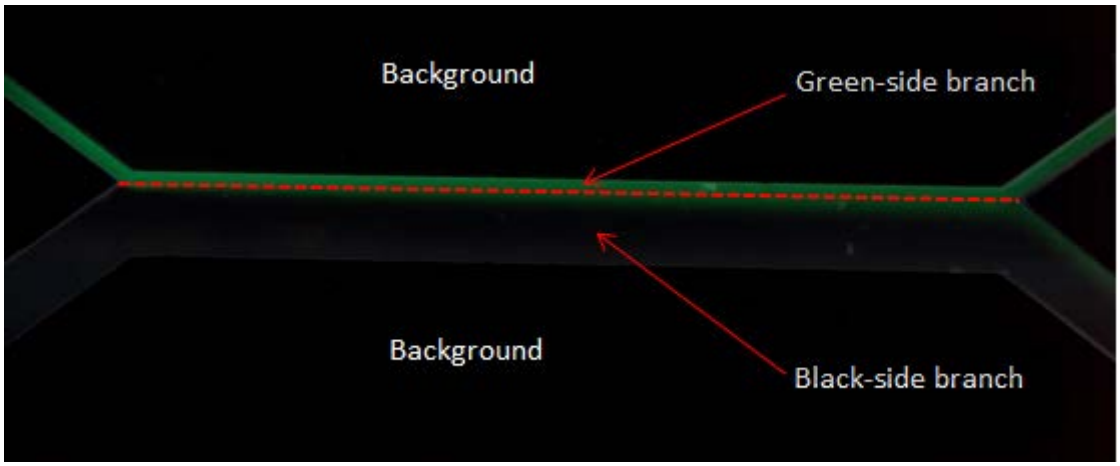

Figure 9. Regions to be distinguished in each photo.

The inhomogeneous illumination of the microscope and the possible contamination due to ambient light were compensated by considering the fluorescence intensity of the background. For that purpose, the background fluorescence intensity value was

subtracted to the fluorescence values taken for the areas located inside the chip (green and black branches). The image analysis was preceded by the sketch of a mesh in each photo in order to analyze the same points in all photos making the results comparable. This sketch is schematized in Figure 10.

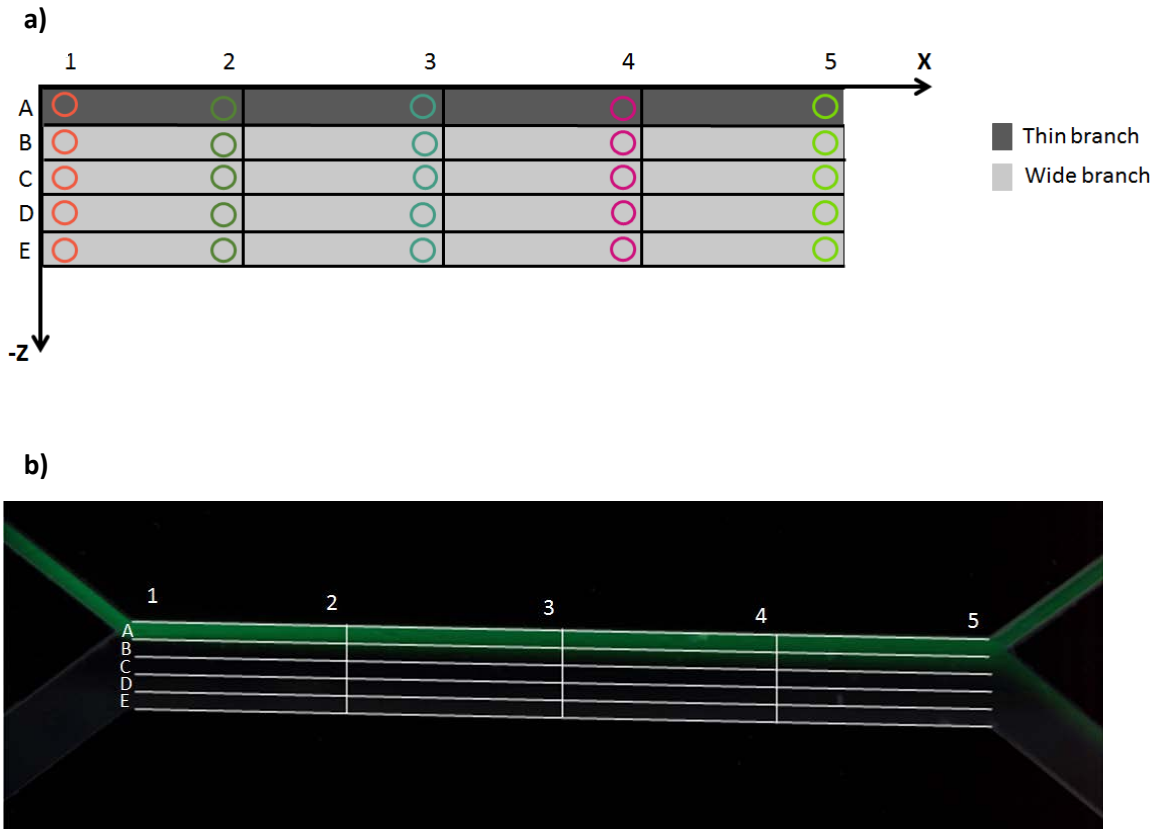

Figure 10. a) Mesh sketch for image analysis; b) Application of the mesh in an experimental image.

In order to represent this mesh, being aware that the widest branch is four times the thinnest one, the microchannel width can be divided in five sections along the Z-axis, which are designated with the letters from A to E. Besides, the chip length is divided in three parts (X-axis), corresponding to the half and the quarter parts which are labelled with numbers from 1 to 5. This way, in each zone of the Z-axis, five measurements will be done with Image J, as it is shown in the figure 10.

Besides, in order to reduce the effects of the different illuminating conditions for each photo and to make the results comparable, the intensity of fluorescence was

represented as a percentage ($\frac{F_{ij}}{F_{1A}}$) being *j* the zones considered in Z-axis and *i* the measurements carried out in each zone along X-axis. Therefore, F_{1A} corresponds to the fluorescence intensity at the system inlet. It is expected that the intensity of fluorescence for j=C,D,E, value is zero (or very low) as this implies that only water flow through this branch. On the contrary, the highest level of fluorescence are expected to be found in zone A (where fluorescein sodium phase flows) followed by zone B.

When working with microchannels, it is expected that fluid inside the chip flow in the laminar regimen. In order to verify this assumption, the Reynolds number was calculated from equation 1, for the experimental conditions considered and reported in Table 1:

$$Re = \frac{\rho_i \, v_i \, D_{hi}}{\mu_i} \qquad (1)$$

Table 1. Design of experiments.

Experiment	v_w (mm/s)	v_f (mm/s)	ΔP_w (Pa)	ΔP_f (Pa)	n (-)
$t_{res} >> t_{diff}$ ➡ n≥1 ; $\Delta P_w = \Delta P_f$					
EXP 1	1.26	0.18	2.55	2.55	4
EXP 2	2.52	0.35	5.1	5.1	2
EXP 3	5.04	0.71	10.2	10.2	1
$t_{res} << t_{diff}$ ➡ n<1					
$\Delta P_w \neq \Delta P_f$					
EXP 4	40	10	81	144	7.08E-02
EXP 5	40	30	81	432	2.36E-02
EXP 6	40	40	81	576	1.77E-02
$\Delta P_w = \Delta P_f$					
EXP 7	10.07	1.42	20.4	20.4	0.5
EXP 8	20.15	2.83	40.8	40.8	0.25
EXP 9	50.37	7.08	102	102	0.1

v_w: water solution velocity; v_f: fluorescein sodium solution velocity; ΔP_w: water solution pressure drop; ΔP_f: fluorescein sodium solution pressure drop; n: ratio of the residence and diffusion time for the fluorescein phase.

where v_i is the velocity considered in each experimental condition; ρ (density) and μ (dynamic viscosity) are assumed to be the same for both fluids: ρ=998 kg/m^3, μ=10^{-3} kg/m·s[35] and D_{hi} is the hydraulic diameter of the volume occupied by the phase i inside the channel (D_{hw}=0.18mm, D_{hf} =0.07mm).

The Reynolds number for all the experimental conditions was in the range 0.01-8.94. These low Reynolds numbers determine that both fluids flow across the microchannel in the laminar regimen. Therefore, viscous forces dominate over inertial forces reducing the flow irregularities that lead to fluid mixing (turbulence). Thereby, this operation conditions are adequate for keeping two adjacent streams of miscible fluids flowing side-by-side across the microchannel without mixing between them.

In the experiments, two different scenarios were studied being the experimental conditions summarized in Table 1 and calculates with the following methodology. In the first one (EXP 1-3), it is expected that the diffusive transport of fluorescein between the phases takes place, as the residence time of the fluorescein in the microdevice is higher than the time required for the fluorescein sodium molecules to diffuse. Thereby, under these experimental conditions, the possibility of the diffusion to take place in the microdevice is verified. In this scenario, the same pressure drop has been assumed in both chip's branches. As the objective is to achieve the co-flowing of miscible fluids with no intermixing between them obtaining two completely separated phases at the system outlet, in the second scenario, unfavorable conditions for the mass transfer has been considered, as in this case the residence time of the fluorescein sodium molecules in the microdevice is lower that the diffusion time. Therefore, it is expected that with these experimental conditions, the fluids intermixing would be minimized and two completely separated streams at the system outlet could be obtained. Besides, in this case, different (EXP 4-6) and equal (EXP 7-9) pressure drop in both chip branches have been considered so as to the influence of the pressure drop on the system performance could be assessed.

In order to analyze the mass transfer between the components of each phase, the diffusion of the fluorescein from the phase *f* to the phase *w* was evaluated. Thus, flowrates for both fluids were calculated for different ratios (n-values) between residence time (t_{res}) and the diffusion time of the fluorescein phase (t_{diff}) (eq. 2):

$$n = \frac{t_{res}}{t_{diff}} \tag{2}$$

t_{diff} was calculated from the Random Walk Model diffusion model.[36] This model, proposes two different equations for the calculation of t_{diff}, taking into account the diffusion phenomena in one (t_{diff}^{1D}) (eq. 3) or two (t_{diff}^{2D}) (eq. 4) dimensions. In equations 2 and 3, l_{diff} is the width of the branch in which the diffusion phenomena takes place, that in chip used in the experiments is l_{diff}= 0.040 mm and *D* is the diffusion coefficient for fluorescein sodium in water ($D_{f/w}$=4.25·10^{-4} mm^2/s)[37].

$$t_{diff}^{1D} = \frac{l_{diff}^2}{D} \tag{3}$$

$$t_{diff}^{2D} = \frac{l_{diff}^2}{2\,D} \tag{4}$$

The fluorescein diffusion was analyzed only in one dimension in this work, however, diffusion phenomena takes place in every spatial dimension. For taking this effect into account, the mean value between the times, calculated from eq. 3 and 4, was used in this work. These t_{diff} and the different n-values listed in Table 1 were used to estimate the residence time of the fluorescein sodium phase from equation 2.

The velocity of the fluorescein phase (v_f) injected to the thinnest branch of the channel was calculated from the length of the chip, L=2 mm and the residence time definition which was established according to the selected values on *n* (eq. 5):

$$t_{res} = \frac{L}{v_f} \tag{5}$$

For EXP 1-3 and 7-9, the same pressure drop was assumed in both chip´s branches, which ideally implies any intermixing at the outlets. In order to precisely calculate the fluid velocities developed inside the channel, and therefore, the pressure drop owing to the flow of the fluids, the Navier-Stokes and the continuity equations should be resolved. However, they are a set of coupled differential equations very difficult to solve, being the approximations to the equations estimated in practice by using CFD (Computational Fluid Dynamics) techniques. However, for the fluidic analysis, the pressure loss developed by each phase inside the chip is a necessary variable to take into account since its value at the outlets determines the occurrence of intermixing between phases. For simplicity, in this work the pressure drop for the phase *i* was estimated from the Hagen-Poiseuille law as follows:

$$\Delta P_i = \frac{32\ \mu_i\ L\ v_i}{D_{hi}^2} \tag{6}$$

Where μ_i is the dynamic viscosity of the phase i, which is assumed to be equal for both of them ($\mu_i=10^{-3}$ kg/m·s)[33]; L represents the length of the chip (L=2mm) and vi and D_{hi} are the velocity of the fluid considered in each case and the hydraulic diameter of the volume occupied by the phase i inside the channel (D_{hw}=0.18mm, D_{hf} =0.07mm), respectively.

If the pressure drop is the same in both chip's branches, the velocity of water inside the chip can be calculated from eq.6 as:

$$v_w = \frac{D_{hw}^2}{D_{hf}^2}\ v_f \tag{7}$$

For EXP 4-6, different ratios between the velocities of both fluids were assessed and therefore equation 6 was used for determining the pressure drop in each chip's branch. The ratios considered were: $\frac{v_w}{v_f} = 4, 1, 1.33$.

Finally, the flowrates of both fluids were calculated using equation 8:

$$Q_i = A_i \cdot v_i \quad (8)$$

where the subindex i represents either water (w) or fluorescein sodium (f) solutions, Q_i is the flow rate of the phase i, Ai represents the cross sectional area of the volume occupied by the phase i inside the microchannel (A_w= 0.032 mm^2, A_f= 0.008 mm^2) and v_i represents the average velocity of the phase i inside the chip.

4. Results and discussion

4.1. Viability of diffusion phenomena in microchannels

The viability of the diffusion phenomena in microchannels was assessed by considering favourable operation conditions for the mass transfer between the fluids involved. Thereby, the ratio between the residence and the diffusion time (n-value) is higher than or equal to 1 (EXP 1-3).

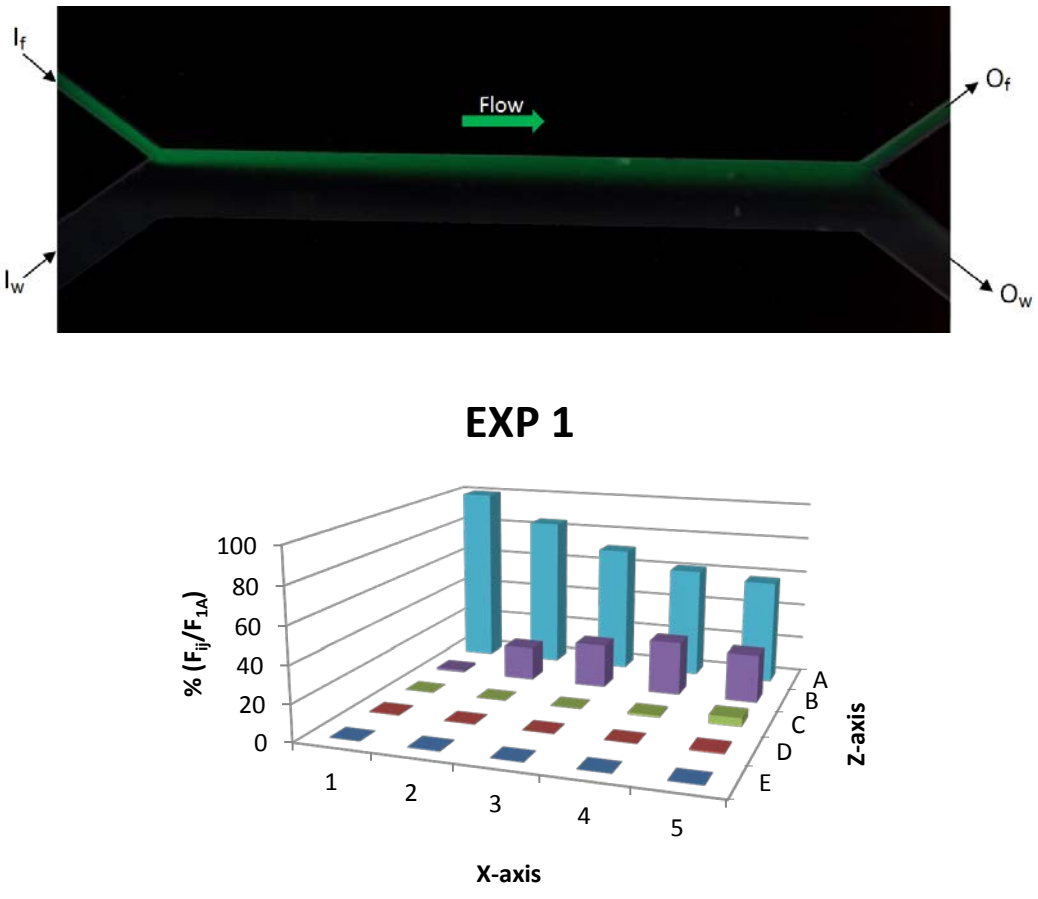

Figure 11. Evolution of fluorescence intensity in the first scenario for n=4.

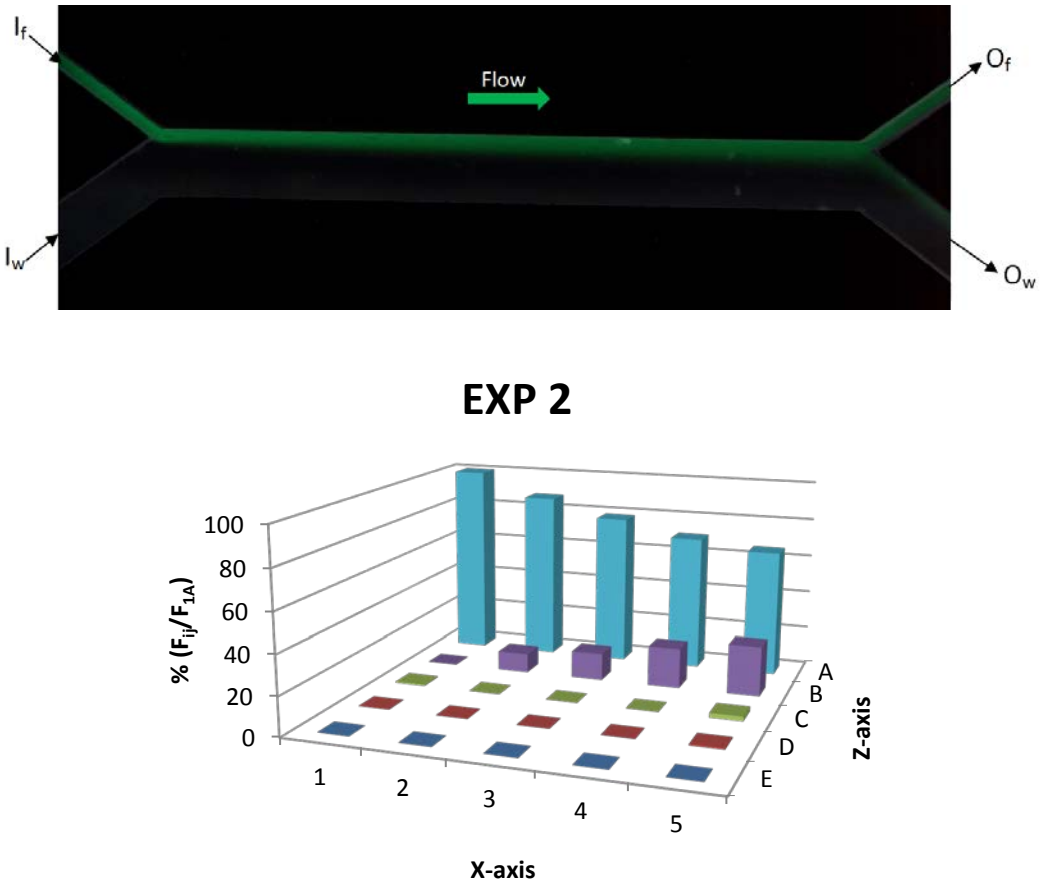

Figure 12. Evolution of fluorescence intensity in the first scenario n=2.

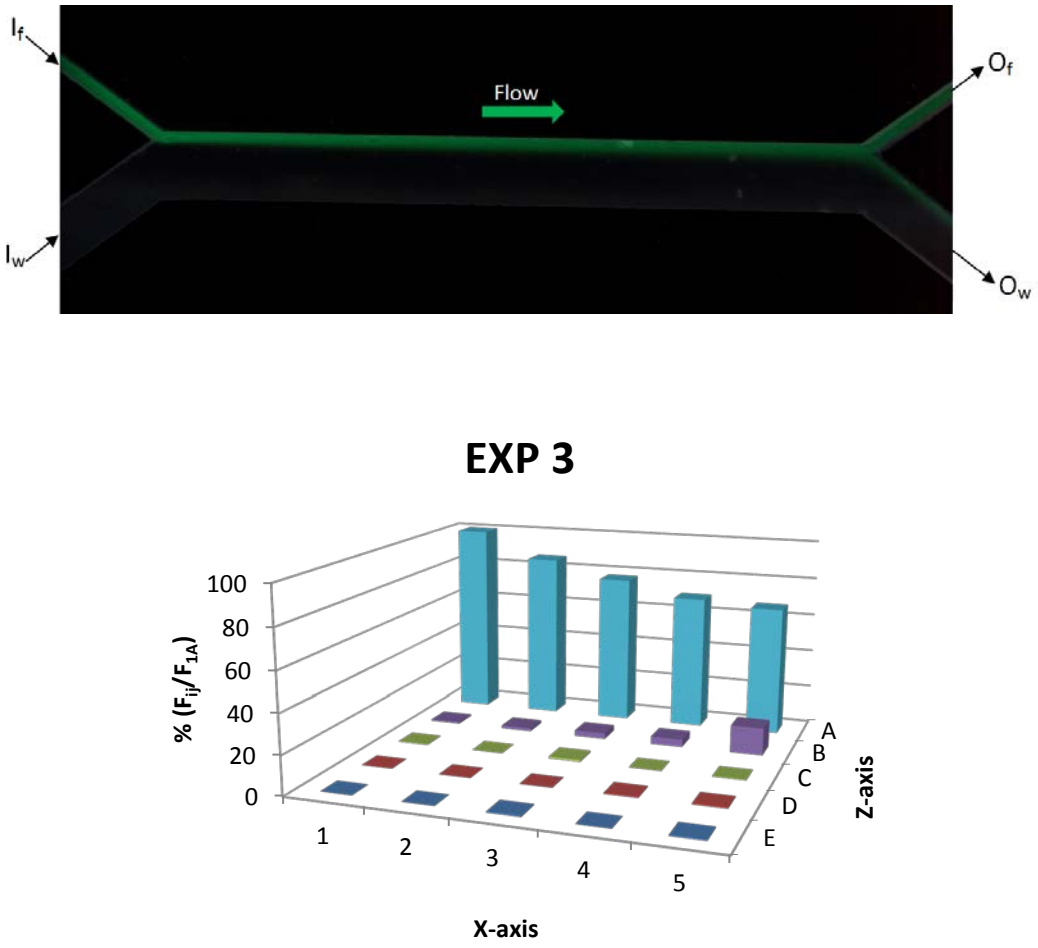

Figure 13. Evolution of fluorescence intensity in the first scenario for n=1.

According to the results reported in Figures 11-13, the diffusion phenomena at the interface between phases takes place, since the fluorescence intensity disclosed in zone A (corresponding to the zone where the fluorescein phase flows) decreases as the fluids move to the system outlet whereas in zone B, the fluorescence level follows the inverse tendency, meaning that the fluorescein concentration in that zone increases along the axial direction of the channel. The reduction of the intensity of fluorescence in zone A is estimated to be 42% for the experimental conditions of Figure 11. On the other hand, for the experimental conditions of Figures 12 and 13, this reduction is approximately of 34%. Regarding to zone B, the increase experimented in each case is around 25% for EXP 1 and 2 and 14% for EXP 3. Also, it can be perceived that the higher the ratio between the residence and the diffusion times (n-value), the higher the amount of fluorescein is being registered in zone B, i.e. the higher the mass transfer between both phases. This

behavior corresponds to the one expected as increasing the n-value, the time that the fluorescein molecules are in the chip increases and therefore, the diffusion is favored. Besides, the diffusion phenomenon is verified by the accomplishment of the mass balance for each measurement (eq. 9).

$$F_{inlet} = \sum_{j=A}^{E} |\Delta F_{ij}| \qquad \forall_i = 1, \dots, 5 \qquad (9)$$

Where F_{inlet} corresponds to the intensity of fluorescence of F_{1A}, the subindex *j* represents the zones considered along the Z-axis and *i* the carried out in each zone along X-axis.

This accomplishment of the mass balance can be noticed from figures 11-13. However, in order to verify this tendency, the mass balance to the fluorescein sodium has been performed for the previous experiments. The results are illustrated in Figure 14-16.

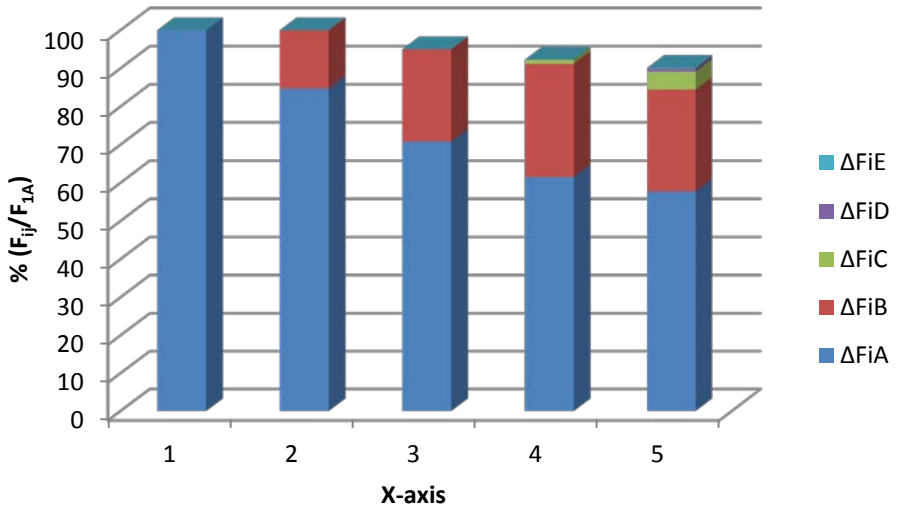

Figure 14. Results of the mass balance for n=4.

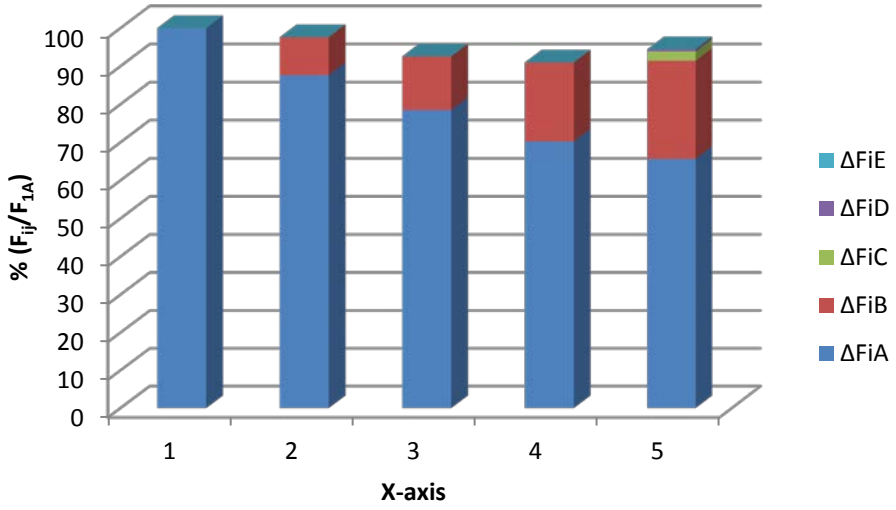

Figure 15. Results of the mass balance for n=2.

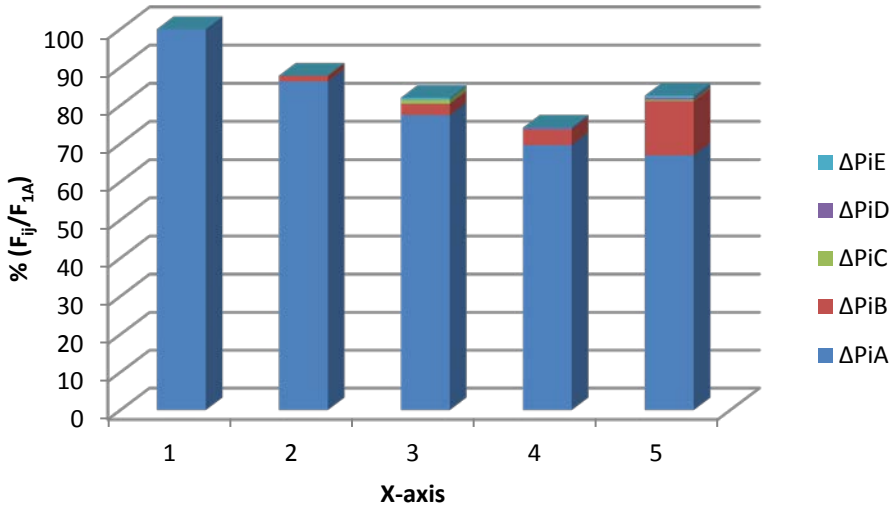

Figure 16. Results of the mass balance for n=1.

According to figures 14-16, the mass balance is accomplished for all the measurements taken in X-axis. The situations in which the mass balance is not fulfilled might be due to the inhomogeneous illuminating conditions of the microscope and the possible experimental error committed during the analysis of the taken photos that hinder the mass balance to be completely fulfilled. The error committed during the photos analysis comes from the difference color conditions of each measurement.

On the other hand, for EXP 1-3, the diffusion is strongly manifest at the system outlet as the larger the microchannel, the larger the residence time for the same fluid velocity and consequently the diffusion phenomena is more appreciated. This perception can be verified from the represented graphs in figure 9 in which the intensity of fluorescence in zone B increases from the inlet to the outlet.

Once the possibility of diffusion in the microdevice has been checked, different operating conditions that lead to minimizing that phenomena are assessed in order to fulfill the coflowing of miscible fluids with negligible mass transfer occurring between them.

4.2. Effect of the pressure drop in the system performance

The effect of the pressure drop in the system performance was evaluated by considering the same and different pressure drop in both chip branches for unfavorable conditions for the mass transfer to occur. Therefore, in this scenario the ratio between the residence and the diffusion time (n-value) is lower than one. The lower the n-value, the lower the expected mass transfer between the fluids involved.

a) Different pressure drop in the microchannel's branches

Figures 17-19 illustrates how the intensity of fluorescence was developed considering different pressure drop conditions.

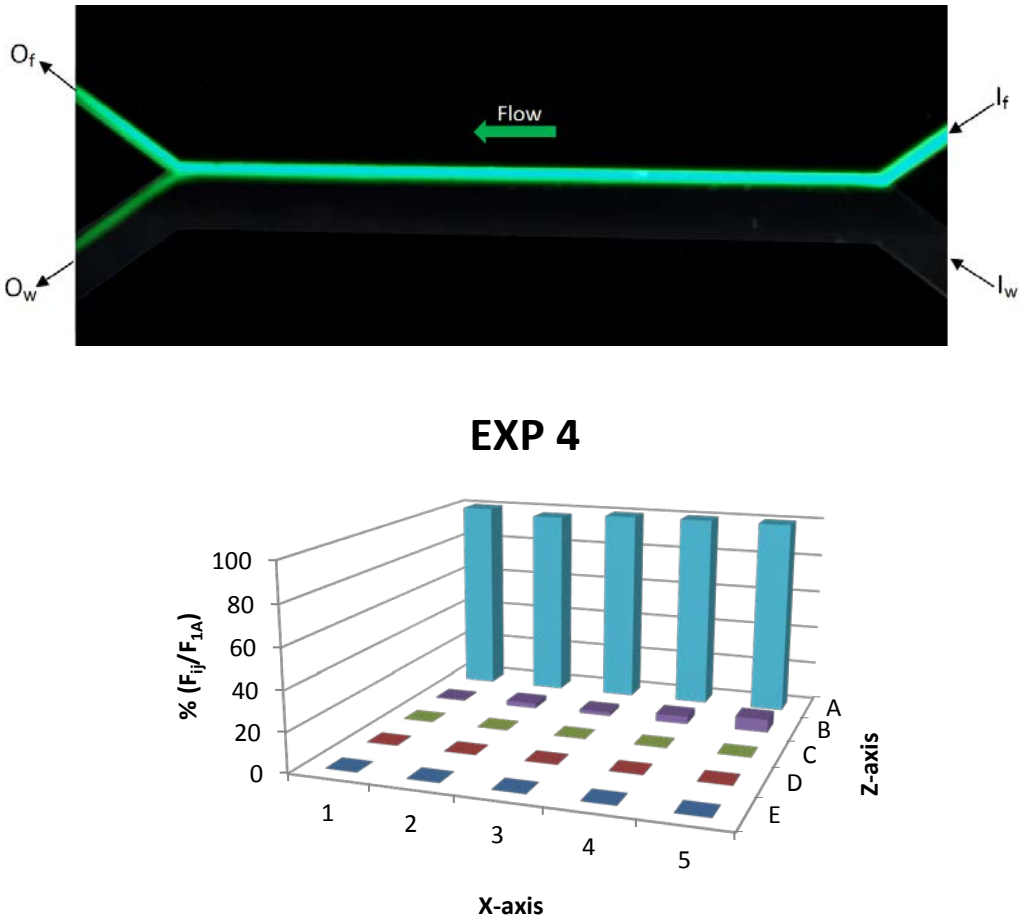

Figure 17. Evolution of fluorescence intensity for the second scenario assuming different pressure drop in the branches: $\frac{\Delta P_w}{\Delta P_f} = 0.6$.

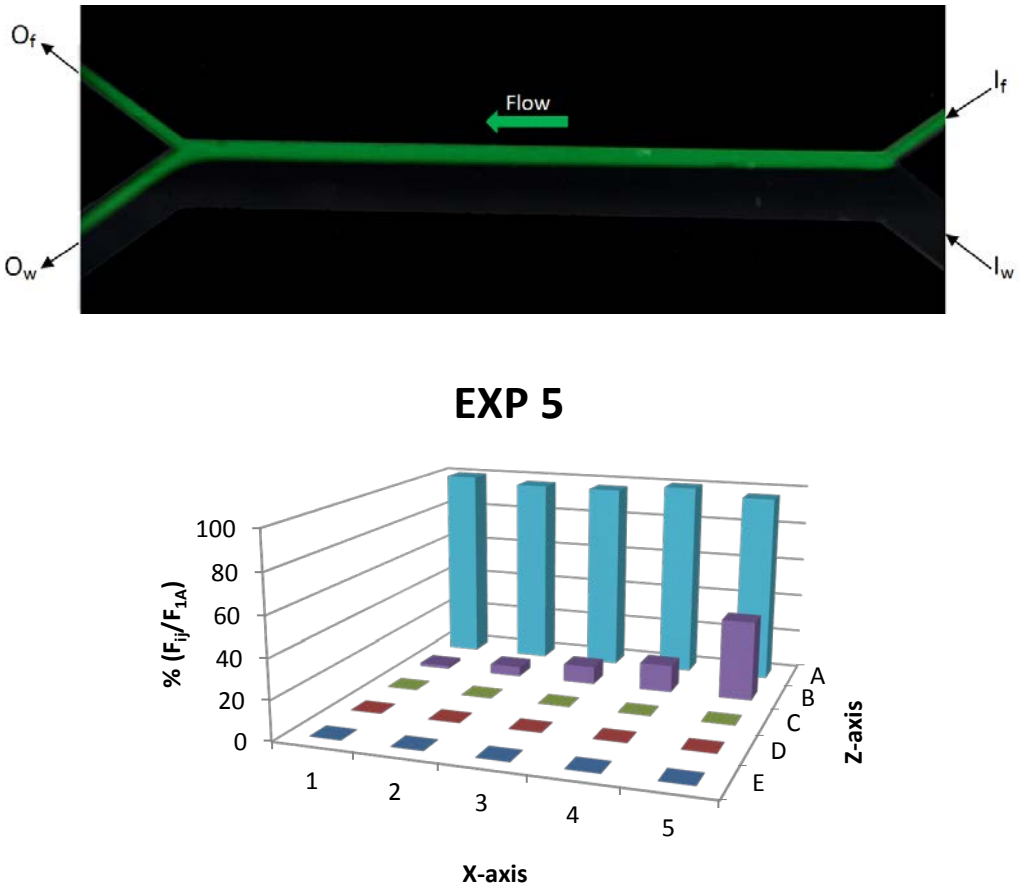

Figure 18. Evolution of fluorescence intensity for the second scenario assuming different pressure drop in the branches: $\frac{\Delta P_w}{\Delta P_f} = 0.2$.

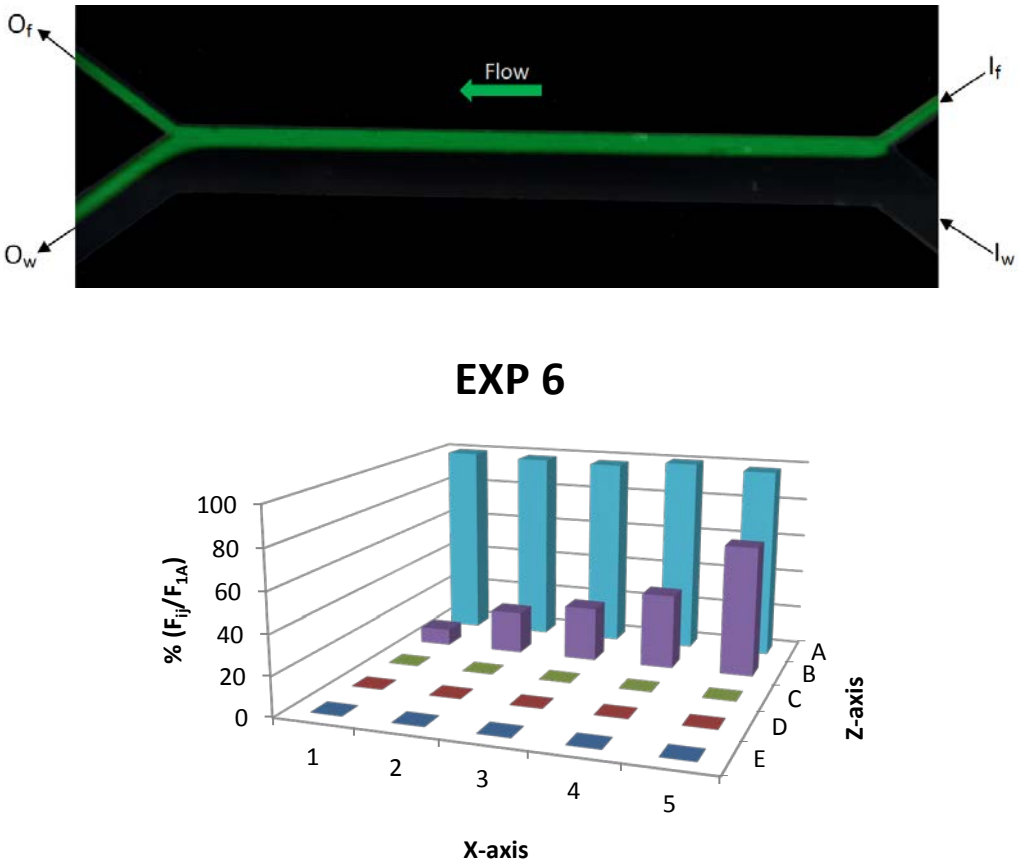

Figure 19. Evolution of fluorescence intensity for the second scenario assuming different pressure drop in the branches: $\frac{\Delta P_w}{\Delta P_f} = 0.1$.

From the graphs included in figure 17-19, it can be noticed that the diffusion phenomena is greatly minimized as the intensity of fluoresce values in the measurements in zone A are the same. The increase of fluorescein in zone B is due to the change in the flow pattern caused by the different pressure drop developed for each phase that lead to the invasion of the fluorescein sodium solution to zone B. Therefore, the lower the ratio of the pressure drop experienced by the phases in the chip's branches, the higher the concentration of fluorescein is reported in zone B. Thereby, the increase of the intensity of fluorescence for figure 17-19 are respectively: 7%, 40% and 60%.However, this is not the result of the diffusion phenomena since the mass balance in this situation is not accomplished (as it was proved for the previous scenario, Figures 14-16). In this case, it was demonstrated that the intensity of fluoresce in zone A is kept constant and the

variation is only appreciable in zone B, whereas in subsequent zones the value of the intensity of fluorescence remains zero.

The operation conditions of experiments 4-6 lead to a well-define interface between both phases and minimize the diffusion phenomena. However, according to the chip's images, a high amount of fluorescein solution elutes the system through the widest outlet as the pressure drop in that branch is lower. This is the result of the high velocities and the different diameter of the branches used in the experiments that favor the elution of the fluorescein phase through the widest branch. Therefore, lower velocities for this phase, i.e. working with the same pressure drop conditions for both phases, will be assessed in order to improve the system performance and to obtain two completely separated phases at the system outlet.

b) Equal pressure drop in the microchannel's branches

Figures 20-22 illustrates how the intensity of fluorescence was developed considering the same pressure drop in both chip's branches.

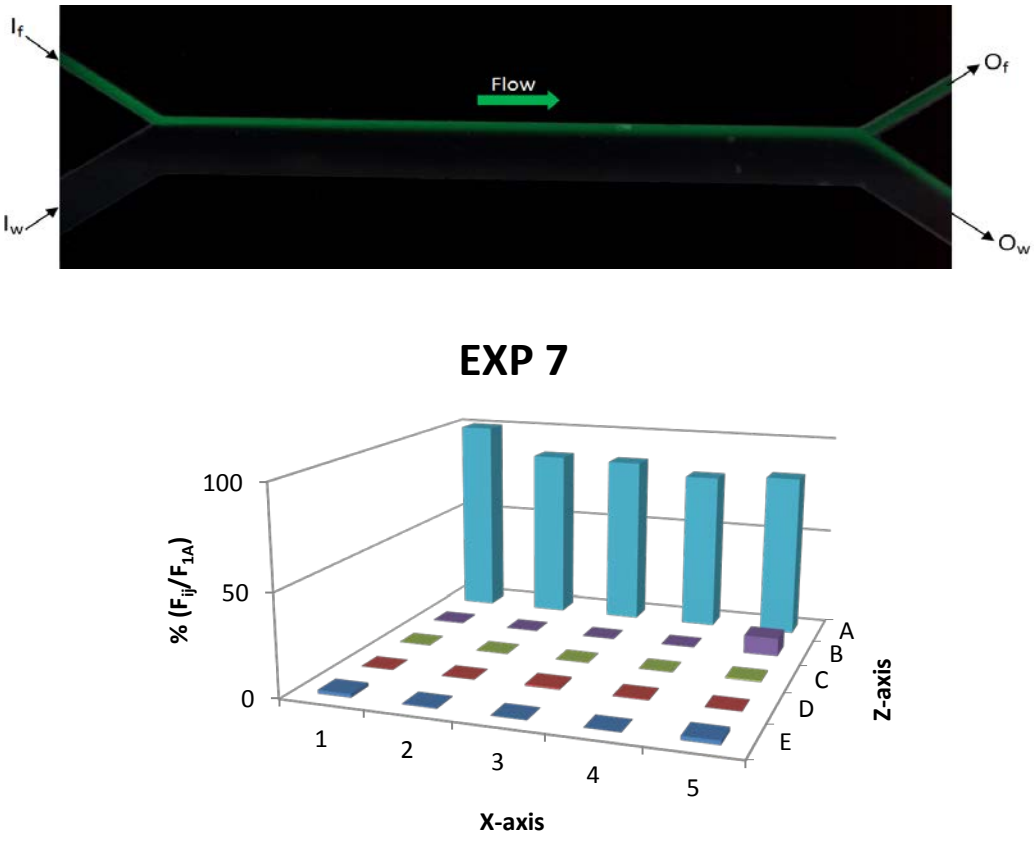

Figure 20. Evolution of fluorescence intensity in the microchannel for the second scenario assuming equal pressure drop in both chip's branches for n=0.5

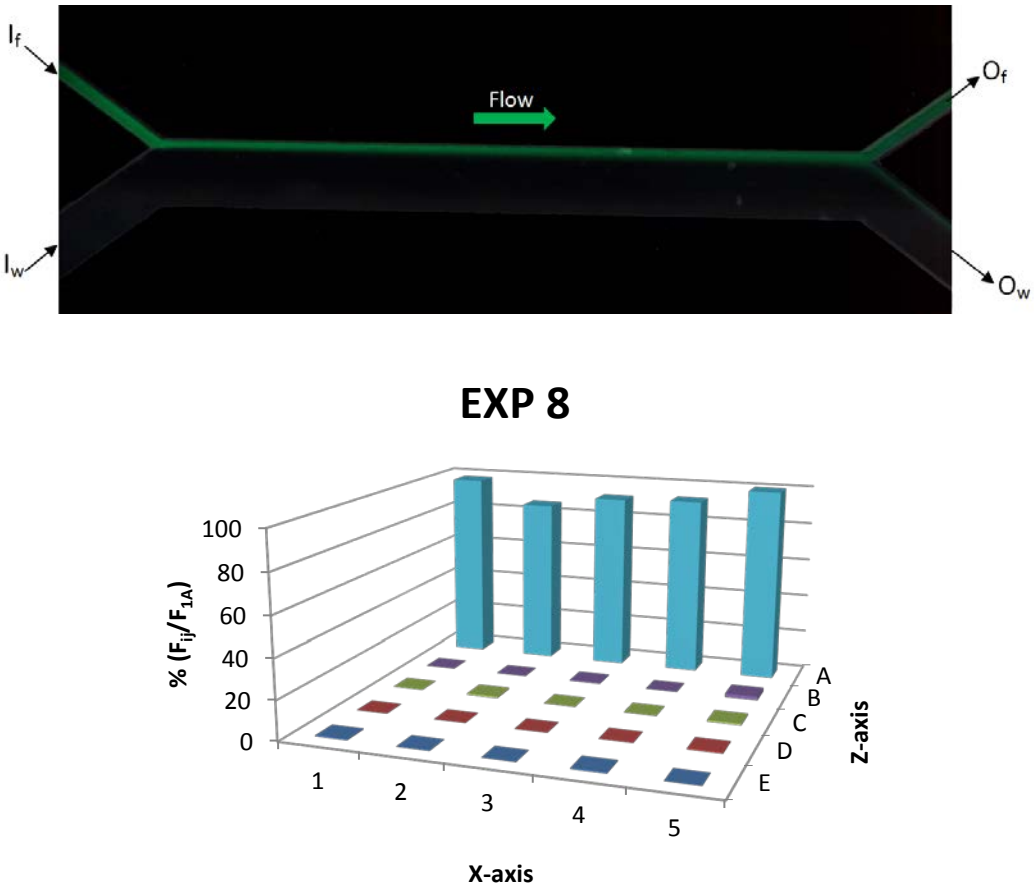

Figure 21. Evolution of fluorescence intensity in the microchannel for the second scenario assuming equal pressure drop in both chip's branches for n=0.25.

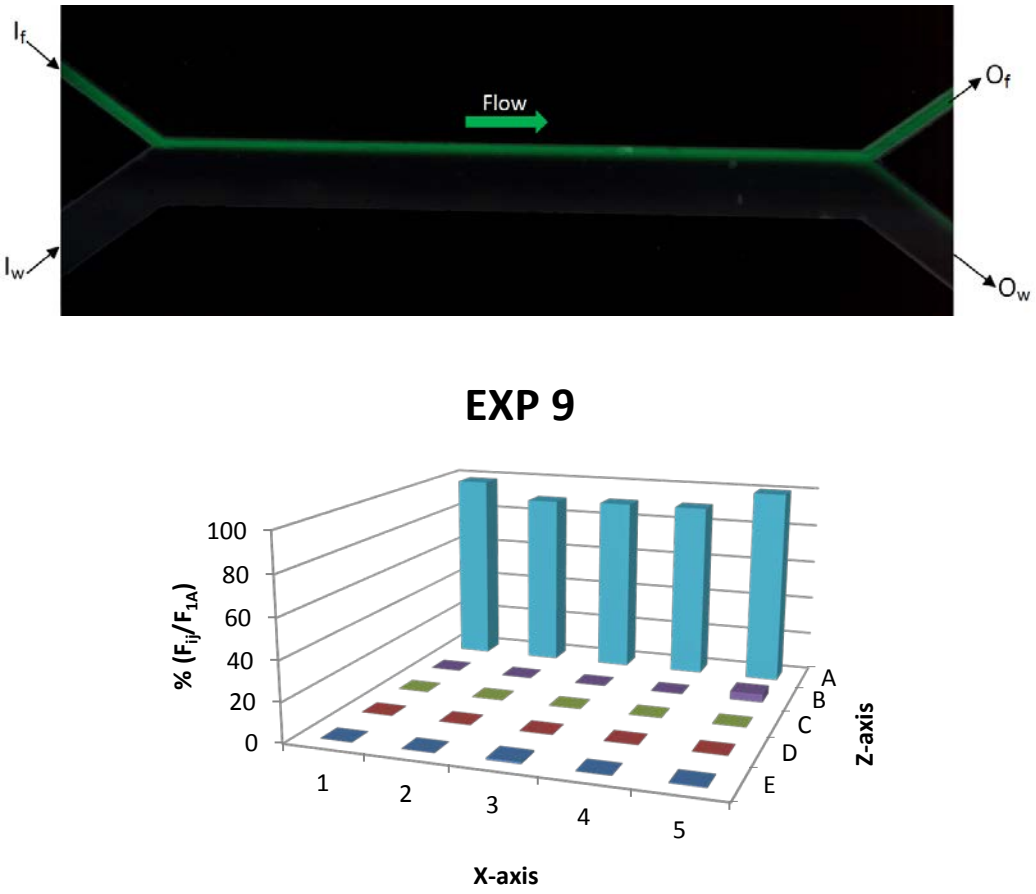

Figure 22. Evolution of fluorescence intensity in the microchannel for the second scenario assuming equal pressure drop in both chip's branches for n=0.1

According to figures 20-22, in which residence higher than diffusion time are considered, diffusion is minimized, since the amount of fluorescein in zone A is kept constant as the fluids move to the system outlet. This behavior is the same as in figures 18-20, since unfavorable conditions for the mass transfer has been considered (n <1). The diffusion has been minimized as the value in zone A is maintained constant and there is no appreciable fluorescein in zone B or the amount is very low and therefore, as in figure 11, the mass balance is not fulfilled.

As in Figures 18-20, the interface between both fluids is well-defined due to the negligible diffusion phenomena under this scenario. However, working with high velocities, the interface between both phases is more well-defined, which implies that the mass transfer between adjacent layers of the fluids is negligible, as the higher the

velocity the lower the residence time, thus decreasing the diffusion but the pressure drop increases. Therefore, a compromise solution must be achieved.

Comparing the chip's images it can be perceived that a substantial reduction in the amount of fluorescein solution that elutes the system though the widest branch has been achieved. Therefore, when maintaining the same pressure drop for both phases, only a thin fluorescein sodium solution film appears at the wall of the widest outlet. Therefore, these operation conditions lead to a better system performance as allow to minimize the loss of fluorescein. This result reveals that when working with the same pressure loss conditions and n values lower than 1, the phase separation is greatly improved. However, the fluorescence reported in the wall of the widest outlet is due to the existence of diffusional transport of molecules between the phases interface. Thereby, water with a little amount of fluorescein sodium was taken at the wide outlet.

Contrasting the first scenario (figure 11-13) and the second scenario for the same pressure drop conditions (figure 20-22), it can be demonstrated that the lower the ratio between the residence and the diffusion time (n-value), the interface between both fluids is more well-defined, which means that the diffusion phenomena, although is taking place, can be neglected. This behavior has been checked by comparing the straight part of the microchannel for EXP 1 and EXP 9 (see Figure 23), where in latter the interface between phases is more well-defined.

Figure 23. Comparison of phases interface for (a) EXP 1 (n=4), (b) EXP 9 (n=0.1).

Additionally, for residence times much lower than diffusion times the decrease in the intensity of fluorescence values as the fluid moves along the microchip is diminished and therefore, the measurements carried out in Zone A have almost the same value. On the contrary, in the $t_{res} >> t_{diff}$ scenario (n >1), the intensity of fluorescence in zone A greatly decreases as the fluorescein sodium moves to the outlet. This different behavior between the scenarios is due to the diffusion phenomena, which is more evident when the n- value increases, as it was expected.

During the performance of the experiments, it has been detected that some of the velocities listed in table 1 were too low to maintain a continuous flow along the channel, i.e. pulse flow, as in sometimes the fluorescence intensity reported in the real monitoring disappeared. Besides, other drawback associated with these low velocities is the limited volumes that can be taken at the system outlet in a reasonable operating time in order to measure the fluorescein concentration and consequently determine the intermixing of fluids in a quantitative way.

The results point out that the best operating condition, that lead to obtaining a more well-define interface between the involved fluids as well as two streams greatly separated at the system outlet is the one corresponding to the experiment 9. The key point lays in establishing the operating conditions that minimize the amount of fluorescein sodium solution that elutes the system though the widest branch as well as the diffusion phenomena across the chip. Although the ratios between both times can be reduced keeping the same pressure drop in both chip's branches in order to fulfill the objectives, it should be taken into account that if the velocities are extremely increased, the flow of fluids in the microdevice is destabilized. Other factor to be considered is the low intrinsic resistance of the microfluidic system to support high pressures, which causes the disconnection of the tygon tubes from the holder.

On the other hand, when working with magnetic nanoparticles, three different considerations must be contemplated in order to establish the best operating conditions that lead to a well system performance. These are: the drag force, which is the resistance of the particle to its motion, the pressure drop of the fluids in each branch and the mass transfer.

From the drag force, it is desired that the velocity of the buffer solution is high in order to increase the drag force for that branch of the channel, whereas for the biological fluid to be treated low velocities are preferred in order to enhance the transference of the magnetic nanoparticles from the biological fluid to the buffer solution. Besides, low pressure drop is required for both fluids in order to minimize the volume of biological fluid that leaves the system through the undesired outlet. Regarding to mass transfer, as the objective is to minimize the diffusion between the fluids, low residence time is target and consequently, low fluid velocities. Therefore, in order to establish the operation condition a compromise solution must be achieved between these factors.

5. Further directions and concluding remarks

This project takes part of a project that aims at the development of continuous microfluidic-magnetophoretic separators for the removal of toxic substances from biological fluids. This work contributes to the design of the magnetic separation stage in order to recover the MNPs in which the target compounds were previously uptaken from the biological fluid. In particular, the separation system's behavior was analyzed in terms of flow patterns and mass transfer of the fluids involved. Therefore, optic analysis methods were developed using fluorescence model compounds, and the best operation conditions that lead to the co-flow of fluids and minimization of the mass transfer between phases were determined.

Working with residence times higher than diffusion time for the fluorescein phase ($n<1$), diffusion takes place, being this phenomena more important when increasing that times ratio. Therefore, in order to avoid the mass transfer between the fluids involved, low ratios between the residence and the diffusion time ($n<1$) were required. In this situation, the influence of the pressure drop developed by both fluids phases was studied.

When working with different pressure drop conditions, the volume of fluorescein that enters into subsequent zones (zones B, C, etc.) to the one where it is expected to flow (zone A) is high as well as the volume of fluorescein solution that elutes the system through the widest outlet. However, working with the same head loss, these effects are

minimized. On the other hand, high velocities (low t_{res}) imply a more constant interface between the phases due to the negligible fluorescein diffusion for n values lower than 1.

From the analysis of the results it can be concluded that low ratios of the residence and the diffusion time for the fluorescein phase ($n<1$) are required. Besides, keeping the same pressure drop in both chip's branches allows to minimize the loss of fluorescein sodium and the invasion of subsequent zones due to change in the flow pattern. Regarding the velocities employed in the experiments, a compromise solution must be achieved as when working with high velocities for this chip design, the interface between the fluids involved is more well-defined, which means that the diffusion of the component in the interface can be neglected but the pressure drop increases destabilizing the system.

Future work is focused on the following strategies:

- Analysis of the separation stage employing fluids with different properties (density and viscosity).
- Study of the separation of MNPs as a function of variables and parameters that affects the efficacy of the separation performance will be studied.
- Comparison of the experimental results with the ones obtained by CFD techniques.
- Integration of the magnetic separation stage and the previous adsorption stage is expected to be fulfilled.

References

1. Susanto, H, et al. 2012. Effect of membrane hydrophilization on ultrafiltration performance for biomolecules separation. *Materials Science and Engineering,* **32** (7), p. 1759-1766.
2. Kang, J. H., et al. 2014. An extracorporeal blood-cleansing device for sepsis therapy. *Nature Medicine*, **20**(10), p. 1211–1216.
3. Herrmann, I. K., et al. 2015. Magnetic separation-based blood purification: a promising new approach for the removal of disease-causing compounds? *Journal of nanobiotechnology*, **13** (1), p. 1-4.
4. *Bio-Resource.* [Web site]. 2011. [Consulted: 29 June 2016]. Available at: http://technologyinscience.blogspot.com.es/2011/09/gel-filtration-chromatography-gf-size.html#.V3jO0vmLTZ6
5. Thermo Fisher SCIENTIFIC. [Web site]. 2016. United States: Thermo Fisher SCIENTIFIC.[Consulted:29 June 2016]. Available at: https://www.thermofisher.com/us/en/home/life-science/protein-biology/protein-biology-learning-center/protein-biology-resource-library/pierce-protein-methods/dialysis-methods-protein-research.html
6. Mohamed Samer (2015). Biological and Chemical Wastewater Treatment Processes, Wastewater Treatment Engineering, Associate Prof. Mohamed Samer (Ed.), InTech, DOI: 10.5772/61250. Available from: http://www.intechopen.com/books/wastewater-treatment-engineering/biological-and-chemical-wastewater-treatment-processes
7. *BIO-RAD*. [Web site]. 2016. [Consulted: 29 June 2016]. Available at: http://www.bio-rad.com/es-es/applications-technologies/introduction-protein-electrophoresis
8. TETALA, K. K. R., Vijayalakshmi, M. A. 2016. A review on recent developments for biomolecule separation at analytical scale using microfluidic devices. *Analytica Chimica Acta*, **906**, p. 7-21.
9. Suen, S.Y., Liu, Y. C., Chang, C. S. 2003. Exploiting immobilized metal affinity membranes for the isolation or purification of therapeutically relevant species. *Journal of Chromatography B*, **797** (1), p. 305-319.

10. Righetti, P.G., Gelfi, C. 2000. Electrophoresis. *Ullmann's Encyclopedia of Industrial Chemistry*, **12**, p. 393-421.
11. Peterson, Z. D., et al. 2003. Advantages and limitations of coupling isotachophoresis and comprehensive isotachophoresis–capillary electrophoresis to time-of-flight mass spectrometry. *Journal of Chromatography A*, **992** (1), p. 169-179.
12. Witek-krowiak, A., et al. 2011. Ultrafiltrative separation of rhamnolipid from culture medium. *World Journal of Microbiology and Biotechnology*, **27** (8), p. 1961-1964.
13. Anspach, F. B.,Hilbeck, O. 1995. Removal of endotoxins by affinity sorbents. *Journal of Chromatography A*, **711** (1), p. 81-92.
14. LI, Q., et al. 2013. A novel ultrafiltration (UF) membrane with controllable selectivity for protein separation. *Journal of Membrane Science*, **427**, p. 155-167.
15. Ledebo, I. 1998. Principles and practice of hemofiltration and hemodiafiltration. *Artificial organs*, **22** (1), p. 20-25.
16. Meyer, T. W., et al. 2005. The clearance of protein-bound solutes by hemofiltration and hemodiafiltration. *Kidney international*, **68** (2), p. 867-877.
17. Schiffl, H. 2011. High-Flux Dialyzers, Backfiltration, and Dialysis Fluid Quality. En *Seminars in dialysis*. Blackwell Publishing Ltd,. p. 1-4.
18. Conrad, S. E. 2006. Hemodialysis and Hemofiltration. ReasearchGate
19. Rimmelé, T., Kellum, J. A. 2011. Clinical review: blood purification for sepsis. *Crit Care*, **15** (1), p. 1-10.
20. Gómez-Pastora, J., Bringas, E., Ortiz, I. 2014. Recent progress and future challenges on the use of high performance magnetic nano-adsorbents in environmental applications. *Chemical Engineering Journal*, **256**, p. 187-204.
21. FURLANI, E. P. 2010.Magnetic biotransport: analysis and applications.*Materials*, **3** (4), p. 2412-2446.
22. Pamme, Nicole. 2006. Magnetism and microfluidics. *Lab on a Chip*, **6**, (1), p. 24-38
23. Furlani, E. P., et al. 2007. A model for predicting magnetic particle capture in a microfluidic bioseparator. *Biomedical Microdevices*, **9** (4), p. 451-463.
24. Niemeyer, C. M.; Mirkin, Chad A. 2004.*Nanobiotechnology: concepts, applications and perspectives*. John Wiley & Sons.
25. Weibel, D. B.; Whitesides, G. M. 2006. Applications of microfluidics in chemical biology. *Current opinion in chemical biology*, **10** (6), p. 584-591.

26. LO, Roger C. 2013. Application of Microfluidics in Bioprocesses. *Journal of Bioprocessing & Biotechniques*, **2012**.

27. Demierre, N. 2008. *Continuous-Flow Separation of Cells in a Lab-on-a-Chip using "Liquid Electrodes" and Multiple-Frequency.* Renaud, director. Thesis, École Polytechnique Fédérale de Lausanne.

28. Lewpiriyawong, N., Yang, C. 2014. Dielectrophoresis field-flow fractionation for continuous-flow separation of particles and cells in microfluidic devices. In *Advances in Transport Phenomena 2011*. Springer International Publishing, p. 29-62.

29. Volpatti, L. R., Yetisen, A. K. 2014. Commercialization of microfluidic devices. *Trends in biotechnology*, **32** (7), p. 347-350.

30. Cetin, B., Özer, M. B., Solmaz, M. E. 2014. Microfluidic bio-particle manipulation for biotechnology. *Biochemical Engineering Journal*, **92**, p. 63-82.

31. Jamshaid, Talha, et al. 2016. Magnetic particles: From preparation to lab-on-a-chip, biosensors, microsystems and microfluidics applications. *TrAC Trends in Analytical Chemistry*, **79**, p. 344-362.

32. BRIGHAM YOUNG UNIVERSITY. [Web site]. [Consulted: 16 June 2016]
Available at: http://www.cleanroom.byu.edu/su8.phtml

33. Perry, R. H., Green, D. W. 1999. *Perry's chemical engineers' handbook*. McGraw-Hill Professional.

34. Reichman, J. 2000.Handbook of optical filters for fluorescence microscopy.*Chroma Technology Corporation*.

35. Levenspiel, O. 2004. *Flujo de Fluidos e Intercambio de Calor*. España: EDITORIAL REVERTÉ

36. Bruus, H. 2008. *Theoretical Microfluidics.* United States: Oxford University Press Inc.

37. Culbertson, C. T., Jacobson, S. C., Ramsey, J. M. 2002. Diffusion coefficient measurements in microfluidic devices. *Talanta*, **56** (2), p. 365-373.